A broad-line nuclear magnetic resonance study of a vinylidene fluoride/trifluoroethylene copolymer

J. Clements*, G. R. Davies and I. M. Ward†
IRC in Polymer Science and Technology, University of Leeds, Leeds LS2 9JT, UK
(Received 14 March 1991; accepted 9 April 1991)

Broad-line nuclear magnetic resonance measurements have been performed for the proton resonance in an oriented 70:30 copolymer of vinylidene fluoride and trifluoroethylene. The spectra show two components with distinctly different linewidths. The broad component is identified with the crystalline regions and the narrow component with the amorphous. An appreciable reversible change in crystallinity with temperature was observed, which could significantly contribute to the pyroelectric response of this material. In addition, measurements through the Curie transition show the increasing libration of the chains prior to the transition, which could also contribute to the pyroelectric response.

(Keywords: nuclear magnetic resonance; copolymer; vinylidene fluoride; trifluoroethylene; structure; crystallinity; pyroelectricity)

INTRODUCTION

We have previously shown[1], using broad-line n.m.r., that a significant part of the pyroelectric response of poly(vinylidene fluoride) (PVDF) could be due to a reversible temperature-dependent crystallinity change. This paper extends our n.m.r. studies to a copolymer of vinylidene fluoride (VDF) with trifluoroethylene (TrFE).

Such copolymers have attracted much attention[2,3], since they can show high piezoelectric and pyroelectric activity in their melt-crystallized form without requiring the mechanical processing usually applied to PVDF. They are also ferroelectric[4] and can show a Curie point well below their melting point. We shall show that broad-line n.m.r. proves to be a useful tool with which to study the Curie transition.

Though a range of compositions is available, the VDF/TrFE copolymer in the mole ratio 70:30 is probably the most technologically important since this composition readily crystallizes in the non-centrosymmetric form but retains a relatively high Curie point. Copolymers with low TrFE content do not crystallize in the required form and those with high TrFE content have lower Curie points and are not therefore as thermally stable. We have therefore restricted our studies to the 70:30 copolymer.

EXPERIMENTAL

Sample preparation and characterization

The copolymer was supplied by Atochem in pellet form. Isotropic sheets of 1 mm thickness were prepared by compression moulding between steel plates at a temperature of 205°C, and immediately quench cooling from the melt, into water at room temperature. Drawn samples were produced by cutting dumb-bells with a central width of 90 mm and a gauge length of 35 mm from these sheets, and drawing in an air oven in an Instron Tensile Machine at a draw temperature of 83°C, and a draw rate of 0.3 mm min^{-1}, to a natural draw ratio of 7:1.

In an attempt to characterize the crystallinity of the samples, differential scanning calorimetry was carried out using a Perkin–Elmer DSC-2. Two broad endothermic peaks were seen in the thermograms of both the isotropic and oriented samples. The lower-temperature peak, at approximately 100°C, is associated with the Curie point transition of the copolymer from its low-temperature form (similar to PVDF form I) to a higher-temperature form. The higher-temperature peak, at approximately 140°C, is due to crystal melting.

Crystallinities were determined in the usual manner by comparing measured enthalpies of fusion with the enthalpy of fusion of the fully crystalline copolymer. This was estimated as 1395 cal mol^{-1} by interpolation between the reported values for PVDF[5] and PTrFE[6] of 1435 and 1300 cal mol^{-1} respectively. A crystallinity value of 0.55 was estimated for the isotropic copolymer and 0.56 for the oriented sample.

As we shall show, it is likely that these values are not reliable measures of room-temperature crystallinity, since there are changes in both the type and degree of crystallinity as the samples are heated. They do, however, serve to characterize the initial state of the samples.

N.m.r. measurements

The n.m.r. measurements were carried out using a Varian DP60 spectrometer operated at 60 MHz. A time-averaging computer was used to add together the signals from several successive sweeps through the spectrum to improve the signal-to-noise ratio.

The drawn copolymer was available as a sheet 85 μm

* Present address: Department of Chemistry, University of Leeds, Leeds LS2 9JT, UK
† To whom correspondence should be addressed

0032-3861/92/081623-07

in thickness. An n.m.r. sample was produced by cutting 4 mm wide sections from this sheet and packing them into a rectangular slot machined into a 6 mm diameter PTFE (polytetrafluoroethylene) rod. The orientation directions of all the sections were kept parallel to each other and perpendicular to the axis of the PTFE rod. The orientation of the sample with respect to the axis of the static magnetic field was varied by rotating the PTFE rod in the n.m.r. spectrometer probe, the angle being measured by a goniometer head attached to the rod. This angle we call γ'. Spectra were recorded for values of γ' in steps of 15° between −30° and +120°.

Since the measured angle γ' usually differed by a small amount from the true angle γ between the static magnetic field and the sample orientation direction, a correction was applied that left the variation of second moment $\langle \Delta H^2 \rangle$ displaying symmetry about 0° and 90°.

The isotropic copolymer took the form of a sheet of material approximately 1 mm in thickness. Small sections were cut from this sheet and packed into a glass tube of internal diameter 4 mm.

The magnetic field sweep was calibrated by observing the sidebands produced by modulating the transmitter frequency at 21.289 kHz and running a spectrum of glycerine. The modulation produced sidebands at 60 MHz $\pm$ n × (21.289 kHz), which appeared at 5 G intervals in the recorded spectrum. The average field interval at which the signal was recorded was about 0.06 G. The modulation amplitude was calibrated by measuring the separation of the maximum and minimum of the derivative signal of a glycerine sample. The values of the second moments were thus corrected for a modulation amplitude of 0.5 G, giving an Andrew correction[7] of 0.06 G^2. Radiofrequency power levels were chosen to be well below those producing saturation by making preliminary measurements at different power levels at all temperatures. A Varian temperature controller was used to maintain temperatures other than ambient.

THEORY

Calculation of crystallinity

The following procedure was developed previously[1] for the decomposition of composite n.m.r. signals into two components, a broad component associated with the rigid crystalline regions and a narrow component associated with the mobile non-crystalline material. In the present case it was assumed that the crystalline regions give rise to an n.m.r. signal that can be considered to be a Pake doublet, associated with the proton pairs in the $-CH_2-CF_2-$ sequence of the vinylidene fluoride fraction of the copolymer, this doublet being broadened by interactions with the single protons in the $-CHF-CF_2-$ sequence of the trifluoroethylene fraction, and by other intermolecular and intramolecular interactions, to give a Gaussian doublet lineshape as proposed by Pranadi and Manuel[8] for isotropic polyethylene. Following the method developed by Pranadi and Manuel, the Gaussian doublet lineshape was defined as follows:

$$Y(\Delta H) = a_1\left[\exp\left(\frac{-(\Delta H - a_2)^2}{2a_3^2}\right) + \exp\left(\frac{-(\Delta H + a_2)^2}{2a_3^2}\right)\right]$$

This represents the superposition of two identical Gaussian lineshapes whose centres are separated by a field interval $2a_2$ and whose individual second moments about their centres are a_3. The area under this composite curve is $(8\pi)^{1/2}a_1a_3$ and the second moment $\langle \Delta H^2 \rangle = a_2^2 + a_3^2$. The variable $\Delta H = H - H_0$, where H_0 is the magnetic field at the centre of the doublet.

This lineshape was fitted to the outer part of the experimental line with a_1, a_2 and a_3 as adjustable parameters, using a least-squares procedure with parabolic extrapolation described by Bevington[9], by minimizing the sum:

$$\chi^2 = \sum \frac{[A_i - Y(\Delta H_i)]^2}{\sigma_i^2}$$

where A_i is the experimental value of the absorption line at the ith point and $Y(\Delta H_i)$ the corresponding value of the Gaussian doublet.

There are often several local minima for χ^2, among which we require the global minimum. The initial values of a_2 and a_3 were chosen by calculating the value of a_2 appropriate to a pair of protons in a CH_2 group and then deriving a_3 from the theoretical second moment for a perfectly oriented copolymer using $\langle \Delta H^2 \rangle = a_2^2 + a_3^2$. With these parameters chosen, the choice of an initial value for a_1 is straightforward. A range of initial values of the a_n was then used to establish the best overall fit using different ranges of the outer part of the absorption line.

Calculation of the rigid lattice second moments for oriented poly(VDF/TrFE) 70:30

As stated above, a knowledge of the second moments for a perfectly oriented copolymer is required in order to decompose the experimentally determined spectra into rigid and mobile components. The second moments may be calculated by the method due to Van Vleck[10]. This requires a knowledge of the spatial coordinates of the resonating nuclei together with certain fundamental constants. The formula for the resonance of one type of magnetic species on a lattice containing two types of magnetic species can be written:

$$\langle \Delta H^2 \rangle = \tfrac{6}{5} I(I+1) g^2 \mu_n^2 N^{-1} \sum_{j>k} r_{jk}^{-6} (3\cos^2 \beta_{jk} - 1)^2 + \tfrac{4}{15} I_f (I_f + 1) g_f^2 \mu_n^2 N^{-1} \times \sum_{j,f} r_{jf}^{-6} (3\cos^2 \beta_{jf} - 1)^2$$

where I and I_f are nuclear spin numbers, g and g_f are nuclear g-factors, μ_n is the nuclear magneton, N is the number of magnetic nuclei over which the sum is taken, r_{jk} and r_{jf} are the lengths of the vectors joining nucleus j with nuclei k and f respectively, and β_{jk} and β_{jf} are the angles between vectors $\boldsymbol{r}_{jk}$ and $\boldsymbol{r}_{jf}$ and the direction of the externally applied magnetic field H.

The anisotropy of n.m.r. second moments can, in general, be expressed in terms of spherical harmonic functions of the polar and azimuthal angles (γ, ϕ_γ) relating the direction of the applied magnetic field to the specimen orientation axes. For transversely isotropic materials the spherical harmonic functions reduce to Legendre polynomials of argument cos γ as described by McBrierty and Ward[11]. For an aligned transversely isotropic structure, the anisotropy of the broad-line

n.m.r. second moment $\langle \Delta H^2 \rangle$ as a function of the angle γ between the axis of the applied magnetic field and the draw direction of the specimen may be written:

$$\langle \Delta H^2 \rangle = \sum_{l=0,2,4} \frac{4\pi a_l}{2l+1} \mu_n^2 Y_{l0}(\gamma) \langle P_{l0}(\cos \Delta) \rangle \times [I_1(I_1+1) g_1^2 S_{l0}^{11} + \tfrac{4}{9} I_2(I_2+1) g_2^2 S_{l0}^{12}]$$

In the above expression, S_{l0} is the lth lattice sum for interactions between like (S^{11}) and unlike (S^{12}) nuclei:

$$S_{l0} = \sum r_{jk}^{-6} Y_{l0}(\theta_{jk})/N$$

the $\langle P_{l0}(\cos \Delta) \rangle$ are averaged orientation distribution functions, the a_l are constants given by:

$$a_0 = 1/5 \qquad a_2 = 2/7 \qquad \text{and} \qquad a_4 = 18/35$$

the Y_{l0} are real spherical harmonics given by:

$$Y_{l0}(\theta) = [(2l+1)/4\pi]^{1/2} P_l(\cos \theta)$$

and P_l are Legendre polynomials defined by:

$$P_0(\cos \theta) = 1 \qquad P_2(\cos \theta) = (3 \cos^2 \theta - 1)/2$$

$$P_4(\cos \theta) = (35 \cos^4 \theta - 30 \cos^2 \theta + 3)/8$$

The calculation of the anisotropy of the second moment $\langle \Delta H^2 \rangle$ is essentially reduced to the calculation of the lattice sums S_{l0}, which can be calculated from a knowledge of the spatial coordinates of the resonating nuclei. For a homopolymer such as PVDF this is straightforward. In a random copolymer, however, we lose the advantages of crystalline regularity.

To overcome this problem we adopted the following procedure. We originally assumed that nuclear coordinates and unit-cell parameters appropriate to form I PVDF as provided by Hasegawa *et al.*[12] and replaced 30% of randomly situated protons in the PVDF lattice with fluorines, with the following constraint: that only one proton in a given $-CH_2-$ unit of the PVDF chain is replaced, in order that we generate $-CHF-CF_2-$ segments. This procedure was carried out a number of times, lattice sums were calculated each time for all interactions inside a sphere of radius 10 Å, and mean values and mean-square deviations were then calculated. Obviously, the expansion of the lattice by the inclusion of the larger fluorine atoms is not accounted for by this procedure. In an attempt to improve the accuracy of the calculations we then repeated the above procedure with the unit-cell parameters given by Tashiro *et al.*[13] for the 55:45 copolymer. The lattice sums for both structures are tabulated in *Table 1*.

Table 1 Structural information and calculated lattice sums

Hasegawa *et al.* unit-cell dimensions
$a = 8.58$ Å, $b = 4.91$ Å, $c = 2.56$ Å
$\alpha = 90°$, $\beta = 90°$, $\gamma = 90°$

Lattice sums for proton–proton interactions
$S_{00} = 0.005\,45 \pm 0.000\,30$
$S_{20} = -0.003\,12 \pm 0.000\,67$
$S_{40} = 0.006\,42 \pm 0.000\,90$

Lattice sums for proton–fluorine interactions
$S_{00} = 0.003\,23 \pm 0.000\,30$
$S_{20} = -0.000\,05 \pm 0.000\,67$
$S_{40} = -0.000\,42 \pm 0.000\,90$

Tashiro and Kobayashi unit-cell dimensions
$a = 8.92$ Å, $b = 5.17$ Å, $c = 2.56$ Å
$\alpha = 90°$, $\beta = 93°$, $\gamma = 90°$

Lattice sums for proton–proton interactions
$S_{00} = 0.004\,56 \pm 0.000\,25$
$S_{20} = -0.001\,88 \pm 0.000\,55$
$S_{40} = 0.005\,57 \pm 0.000\,74$

Lattice sums for proton–fluorine interactions
$S_{00} = 0.002\,58 \pm 0.000\,25$
$S_{20} = -0.000\,16 \pm 0.000\,55$
$S_{40} = -0.000\,21 \pm 0.000\,74$

RESULTS AND DISCUSSION

General nature of the results

Figure 1 shows the room-temperature derivative and absorption spectra respectively for the oriented sample with the magnetic field aligned parallel to the draw direction and *Figure 2* shows the equivalent spectra for an isotropic sample. *Figure 3* shows the spectra obtained for the oriented sample at $-50°C$.

These spectra are similar to those obtained for the PVDF homopolymer. At room temperature the signal is a composite signal consisting of a broad component and a narrow component. At $-50°C$ the spectrum can be seen to be a broad doublet and the splitting is appropriate to that for proton pairs in the CH_2CF_2 sequence. As

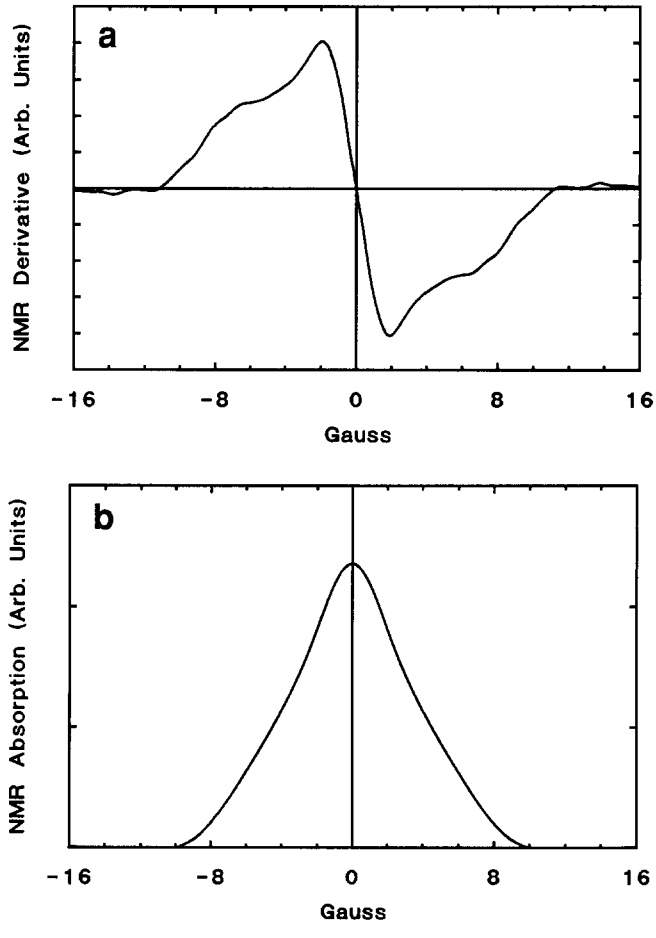

Figure 1 Broad-line n.m.r. spectra for the oriented copolymer at $\gamma = 0°$ and $T = 20°C$: (a) derivative, (b) absorption spectrum

$-50°C$ is well below the glass transition temperature of 0°C, any chain mobility will be quenched and the polymer will show a rigid structure. Under such conditions the major contributions to the second moment, which arise from intramolecular interactions, will be similar for the

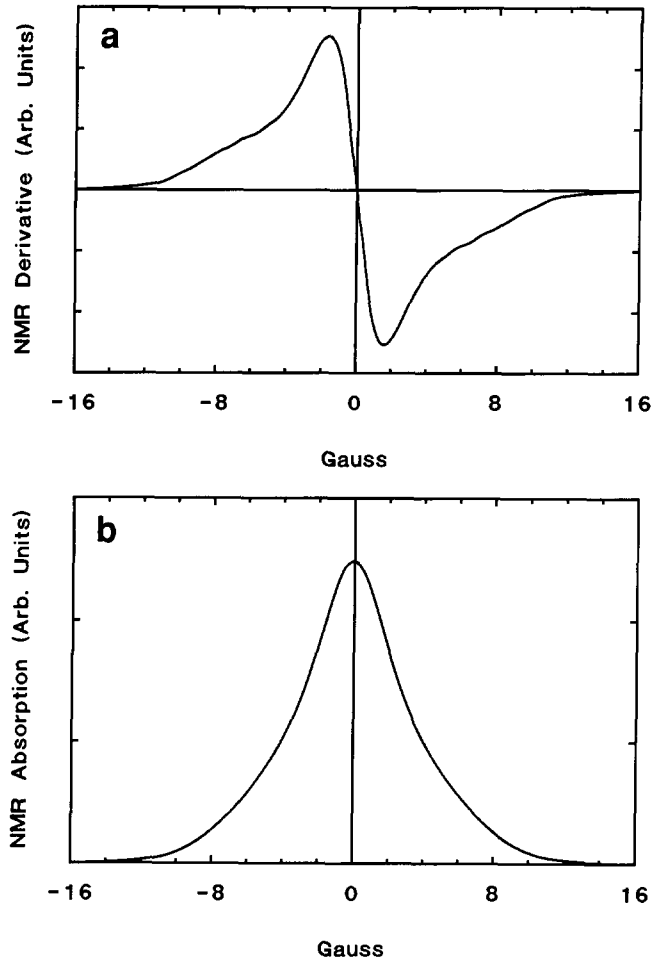

Figure 2 Broad-line n.m.r. spectra for the isotropic copolymer at $T = 20°C$: (a) derivative, (b) absorption spectrum

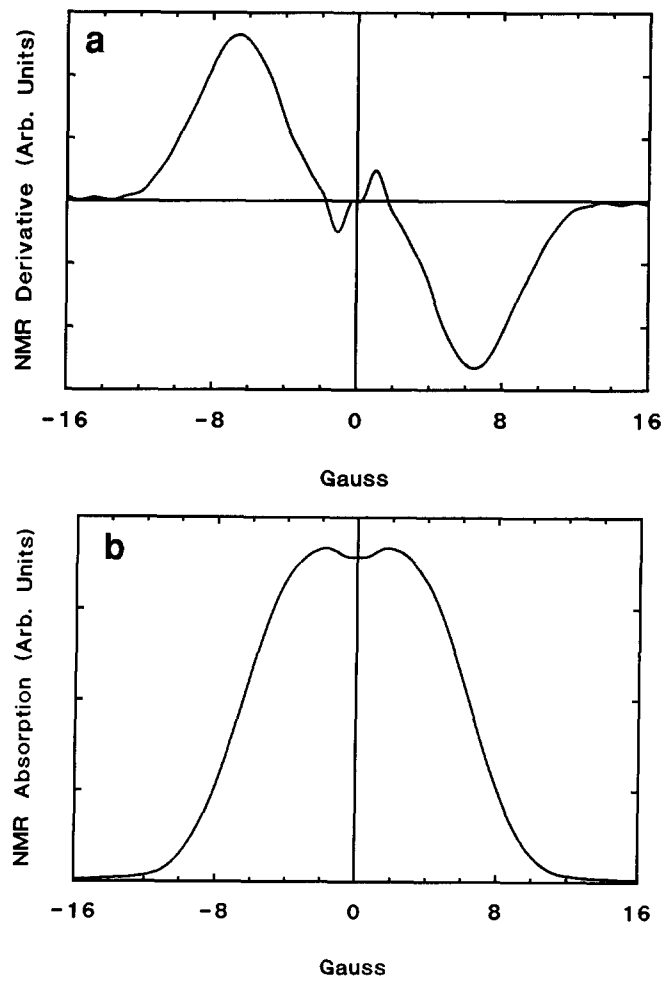

Figure 3 Broad-line spectra for the oriented copolymer at $\gamma = 0°$ and $T = -50°C$: (a) derivative, (b) absorption spectrum

crystalline and amorphous material. In *Figure 4* the second moment anisotropy at $-50°C$ is compared with the predicted anisotropy for a fully oriented sample calculated from the data of Hasegawa *et al.* and Tashiro *et al.* We also show the best fit obtained using the Tashiro lattice sums and values of $P_2(\cos\Delta)$ and $P_4(\cos\Delta)$ optimized for the best fit. A good fit is obtained for the physically reasonable values of $P_2(\cos\Delta)$ and $P_4(\cos\Delta)$ given in *Table 2*.

Determination of the rigid mass fraction

The rigid mass fraction f_R was determined from the spectra for both the oriented and the isotropic samples at each temperature by calculating the ratio of the integrated intensity of the rigid fraction component to the total integrated intensity. The spectra at each temperature were decomposed as accurately as possible by suitably varying the choice of the initial values of the fitting parameters a_n as described above. Since the doublet structure of the rigid fraction is better resolved at $\gamma = 0°$, these results were used as a guide to facilitate the decomposition of spectra at other values of γ. (This better resolution is due to the fact that the proton–proton vector in $-CH_2-$ groups is closely perpendicular to the magnetic field when $\gamma = 0°$.)

The results of the Gaussian doublet fitting procedure for the oriented sample together with numerical values for the rigid fraction f_R are tabulated in *Table 3*. Equivalent results for the isotropic sample are tabulated

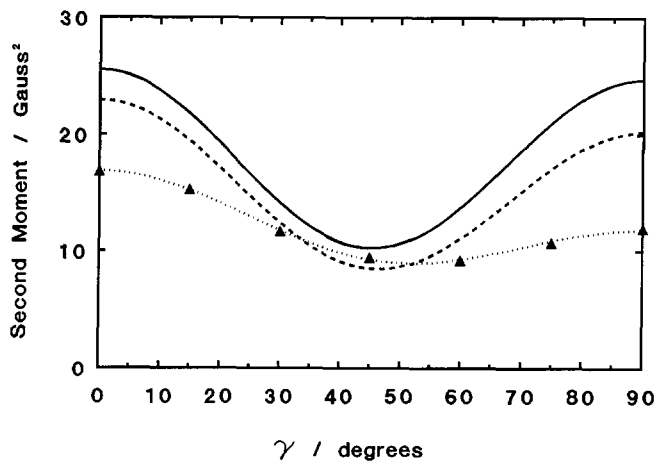

Figure 4 Variation of the proton second moments $\langle \Delta H^2 \rangle_c$ for crystalline copolymer with ideal c axis orientation along the draw direction and transverse isotropy: (——) from data of Hasegawa *et al.*; (– – –) from data of Tashiro and Kobayashi; (▲) experimental data measured at $-50°C$

Table 2 Average orientation distribution functions for drawn poly-(VDF/TrFE) 70:30 estimated from n.m.r. measurements

$\langle P_2(\cos\Delta)\rangle = 0.859$
$\langle P_4(\cos\Delta)\rangle = 0.840$
$\langle \cos^2\Delta\rangle = 0.906$
$\langle \cos^4\Delta\rangle = 0.883$

Table 3 Fitting parameters for Gaussian doublet and rigid fraction values f_R (drawn sample)[a]

T (°C)	γ	a_1	a_2	a_3	$\langle\Delta H^2\rangle$	f_R
20	0	0.051	2.50	3.18	16.35	0.81
	45	0.060	1.69	2.62	9.71	0.79
	90	0.056	1.96	2.81	11.72	0.80
40	0	0.045	2.84	2.91	16.50	0.75
	45	0.068	0.68	1.88	4.00	0.74
	90	0.051	1.61	2.50	8.87	0.74
60	0	0.047	2.56	2.86	15.86	0.68
	45	0.073	0.58	1.81	3.63	0.67
	90	0.045	1.34	2.55	8.33	0.66
80	0	0.046	2.73	2.85	15.58	0.64
	45	0.076	0.57	1.66	3.10	0.64
	90	0.053	1.30	2.40	7.36	0.63
100	0	0.056	2.04	2.09	8.58	0.59
	45	0.076	0.56	1.49	2.86	0.57
	90	0.056	1.29	2.03	6.90	0.57
110	0	0.060	1.93	1.89	7.00	0.57
	45	0.077	0.56	1.47	2.83	0.57
	90	0.056	1.29	1.99	6.85	0.56

[a]Each value quoted is the mean of five measurements. The standard errors in the mean values of a_1, a_2 and a_3 are 3%. The standard errors in the values of $\langle\Delta H^2\rangle$ and f_R are 2%

Table 4 Fitting parameters for Gaussian doublet and rigid fraction values f_R (isotropic sample)[a]

T (°C)	a_1	a_2	a_3	$\langle\Delta H^2\rangle$	f_R
20	0.059	2.32	2.66	12.46	0.79
40	0.050	2.16	2.80	12.54	0.68
60	0.045	2.22	2.78	12.69	0.64
80	0.044	2.20	2.76	12.48	0.61

[a]Each value quoted is the mean of five measurements. The standard errors in the mean values of a_1, a_2 and a_3 are 3%. The standard errors in the values of $\langle\Delta H^2\rangle$ and f_R are 2%

in *Table 4*. The closeness of the values obtained for the rigid fraction at all values of γ is further support for the validity of the procedure used, despite the relatively poor resolution of the two components.

The variation of the rigid mass fraction with temperature is shown in *Figure 5* for both isotropic and oriented samples. We see that the rigid mass fraction decreases with increasing temperature in both cases. The changes were found to be quite reversible provided that the oriented sample was not heated above its draw temperature of 83°C. Above this temperature, significant changes took place in the nature of the spectra, which will be discussed later.

If, as we believe, the rigid mass fraction is a measure of crystallinity, then we must reconcile the apparent discrepancy between the values of about 0.55 deduced from d.s.c. and 0.8 deduced from n.m.r. In fact, no such discrepancy exists since the highest-temperature n.m.r. rigid fraction is about 0.56, in agreement with the d.s.c. data. We therefore conclude that the d.s.c. technique does not accurately measure room-temperature crystallinity. The difficulty arises in drawing a baseline when the crystallinity is slowly changing over a wide range of temperatures. Generally, only the high-temperature region within a few tens of degrees of the final melting point is used, and a high-temperature value of the crystallinity therefore results.

Temperature dependence of the second moment anisotropy

The variation with γ of the second moments of the rigid component is shown in *Figure 6* for temperatures of -50, 20, 60 and 100°C. Also shown is the total second moment at -50°C. At 20°C the rigid fraction second moment is very similar to the total second moment at -50°C. This is consistent with the 'freezing' of the oriented amorphous fraction below T_g to give a broad line similar to the crystalline component. Since the crystallinity is high and there is also an appreciable degree of amorphous orientation, it is not unreasonable that the total spectrum at -50°C is similar to that of the rigid fraction at 20°C.

It is of particular interest that the Gaussian second moment parameter a_3 and separation parameter a_2 (listed in *Table 3*) show little variation with temperature when measured parallel to the magnetic field ($\gamma = 0°$) but both show considerable variation at $\gamma = 45°$ and $\gamma = 90°$. This is reflected in the behaviour of the second moment, which, as seen in *Figure 7*, reduces with increasing temperature from 20 to 80°C at $\gamma = 45°$ and 90° but remains essentially constant at $\gamma = 0°$.

These results reflect the fact that the intramolecular interactions are almost invariant with temperature below 100°C whereas the intermolecular interactions are not. A possible explanation is that the molecular chains

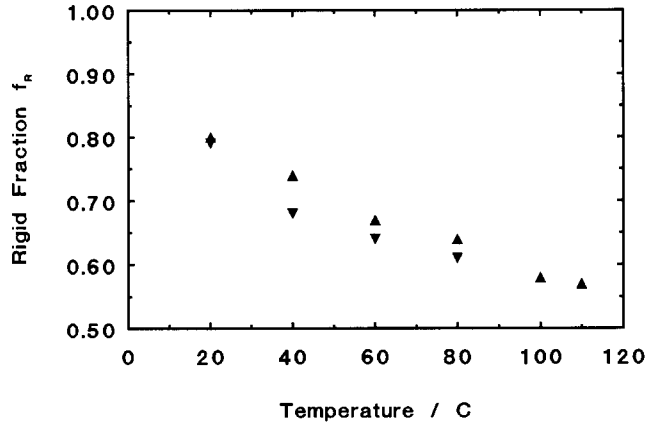

Figure 5 The variation of the rigid mass fraction f_R with temperature: (▲) oriented sample; (▼) isotropic sample

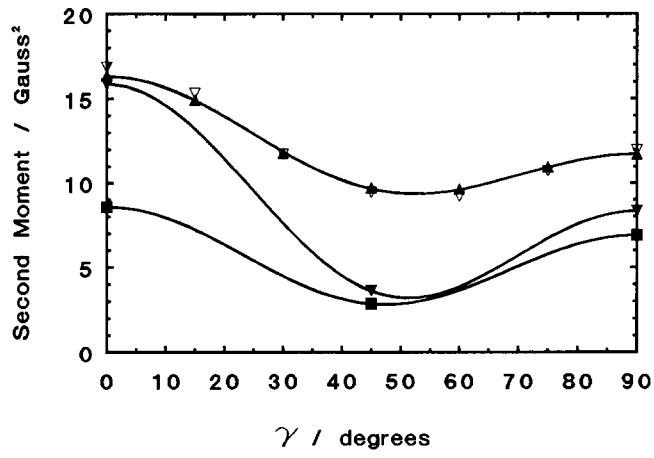

Figure 6 Variation of the second moment of the rigid component of the oriented copolymer with γ at different temperatures: (▲) 20°C, (▼) 60°C, (■) 100°C; (▽) total second moment at -50°C

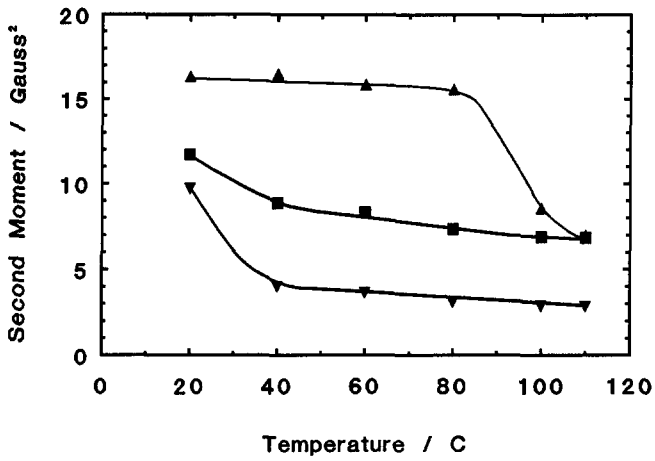

Figure 7 Variation of the second moment of the rigid component of the oriented copolymer with temperature at different values of γ: (▲) $\gamma = 0°$, (▼) $\gamma = 45°$, (■) $\gamma = 90°$

undergo considerable libration about the c axis of the unit cell as the temperature is raised. This reduces the intermolecular interactions but does not affect the intramolecular interactions. Drawing on the theoretical calculations made by Folkes and Ward[14] for the effects of molecular motion on the second moment anisotropy of drawn polyethylene, and the earlier work of Andrew[15] on hydrocarbons, we have been able to estimate the amplitude of libration as follows: at 40°C, ±20° of arc; at 60°C, ±22° of arc; and at 80°C, ±25° of arc.

Above 80°C a marked decrease in the second moment of the rigid component occurs at $\gamma = 0°$. (Though the rigid component is appreciably mobile at these temperatures, there is still a good distinction between the rigid and the mobile phases as seen in *Figures 8a* and *8b*, which show the spectra at 100°C.) This decrease in second moment at $\gamma = 0°$ is due to the change in chain conformation at the Curie transition, the all-*trans* conformation changing to a combination of *TG*, *TG'*, T^3G and T^3G' sequences[16].

Comparison with earlier work on PVDF

In a previous publication[1], we published the results of a similar study on the broad-line n.m.r. behaviour of drawn PVDF. There it was found that PVDF form I displays a similar, though somewhat smaller, decrease in rigid mass fraction with increasing temperature. We also estimated values for the orientation distribution functions for the rigid fraction, $\langle P_2(\cos\theta)\rangle$ and $\langle P_4(\cos\theta)\rangle$, from n.m.r. measurements, and directly from X-ray diffraction measurements. It was found that the agreement between the two was very good indeed. The measure of agreement between the orientation averages indirectly estimated from n.m.r. measurements and directly estimated from X-ray measurements provided further confidence in the decomposition procedure, and the values of the rigid mass fraction. It also led us to suggest that the rigid fraction can be identified with the crystalline regions. By analogy therefore, we propose that the rigid fraction in the copolymer can also be identified with crystalline regions, and that it is possible to estimate orientation averages for this material by this method, which we have done.

As reported above, the change in second moment with temperature implies increasing amplitude of libration of the crystalline copolymer chains with temperature. It is interesting to note that this effect is not seen for the homopolymer in this temperature range, the second moment at all values of γ remaining essentially the same at room temperature and 80°C. The increasing libration in the copolymer may therefore be seen as a precursor for the Curie transition where the structure transforms to a hexagonal 'rotator phase'[16].

Contributions to pyroelectricity

The increasing librational motion of the chains detected here is a major contribution to the primary pyroelectric response and thermal expansion is an important secondary contribution. In addition, the change in crystallinity with temperature, as seen in our earlier paper on PVDF[1], can provide a further important mechanism. The following simple model helps to understand and to quantify these effects.

Imagine a parallel-plate sample of area A and thickness t with N dipoles, each of moment μ making an angle θ_i with the normal to the plate. The polarization P (dipole moment per unit volume) will be given by:

$$P = \sum_i \mu \cos(\theta_i)/At = N\mu\langle\cos(\theta)\rangle/At$$

where $\langle\cos(\theta)\rangle$ is the average value of $\cos(\theta)$.

If we now allow the sample to be a simple two-phase lamellar stack, then it may be assumed that the N_c

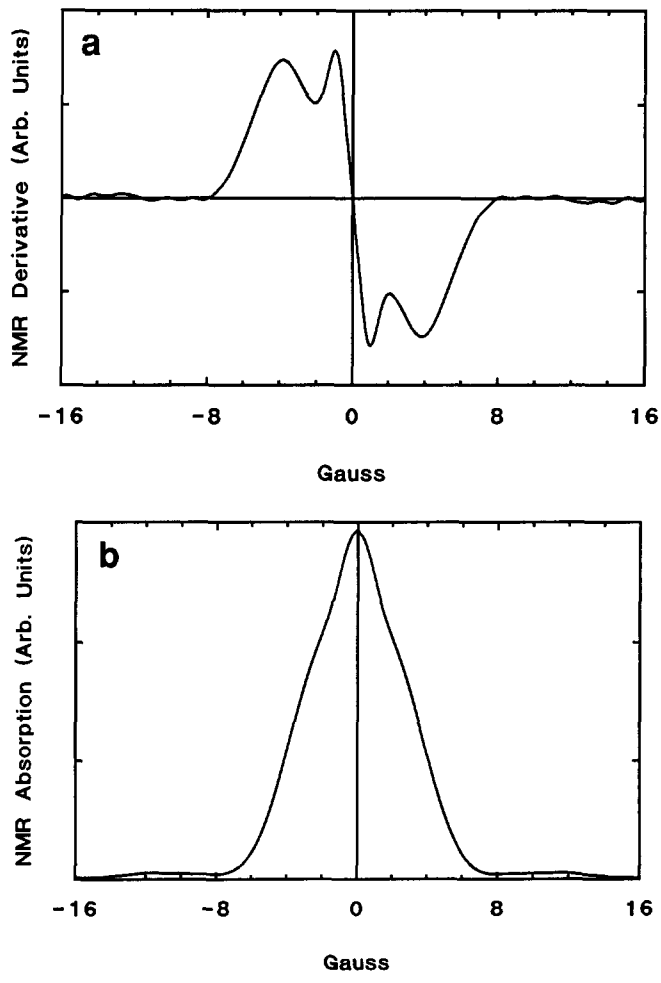

Figure 8 Broad-line n.m.r. derivative spectra for the oriented copolymer at $\gamma = 0°$ and $T = 100°C$: (a) derivative, (b) absorption spectrum

crystalline dipoles are oriented with an average orientation given by $\langle\cos(\theta)\rangle_c$ but that the N_a amorphous dipoles (well above their T_g) point randomly to give $\langle\cos(\theta)\rangle_a = 0$, hence:

$$N\langle\cos(\theta)\rangle = N_c\langle\cos(\theta)\rangle_c + N_a\langle\cos(\theta)\rangle_a$$
$$= N_c\langle\cos(\theta)\rangle_c$$

The charge on the electrodes Q is then given by:

$$Q = AP = N_c\mu\langle\cos(\theta)\rangle_c/t$$

A change in charge (i.e. an observed pyroelectric response) is therefore seen when t, $\langle\cos(\theta)\rangle$, or N_c change with temperature. The change in thickness is thermal expansion, the change in $\langle\cos(\theta)\rangle_c$ can be caused by increasing libration and the change in N_c is a change in mass crystallinity.

Note that all these contributions act to reduce the charge as the temperature is increased, i.e. they all act to produce a negative pyroelectric coefficient.

To quantify these effects we note that the experimental pyroelectric coefficient Υ is given by:

$$\Upsilon = \frac{1}{A}\left(\frac{\partial Q}{\partial T}\right)$$
$$= -\frac{N_c\mu\langle\cos(\theta)\rangle_c}{At^2}\left(\frac{\partial t}{\partial T}\right) + \frac{N_c\mu}{At}\left(\frac{\partial\langle\cos(\theta)\rangle_c}{\partial T}\right)$$
$$+ \frac{\mu\langle\cos(\theta)\rangle_c}{At}\left(\frac{\partial N_c}{\partial T}\right)$$
$$= -P\left[\frac{1}{t}\left(\frac{\partial t}{\partial T}\right) - \frac{1}{\langle\cos(\theta)\rangle_c}\left(\frac{\partial\langle\cos(\theta)\rangle_c}{\partial T}\right)\right.$$
$$\left. - \frac{1}{N_c}\left(\frac{\partial N_c}{\partial T}\right)\right]$$

The polarization P of samples poled at 100 MV m^{-1} has been measured by integrating the thermally stimulated depolarization (TSD) curve and found to be 35 mC m^{-2}. Such samples have a thickness thermal expansion coefficient of 230×10^{-6} K^{-1} and a measured pyroelectric coefficient Υ of -30 μC m^{-2} K^{-1} (ref. 17). The first term in the above equation would predict a contribution of only -8 μC m^{-2} K^{-1} from thermal expansion effects, clearly indicating the operation of other mechanisms.

The increase in libration amplitude from $\pm 20°$ at 40°C to $\pm 25°$ at 80°C allows us to estimate the second term inside the brackets as -4.4×10^{-4} K^{-1}, giving a contribution to Υ of -15 μC m^{-2} K^{-1}. This, together with the thermal expansion term, yields a total of -23 μC m^{-2} K^{-1}, somewhat less than the observed -30 μC m^{-2} K^{-1}.

If we equate the rigid fraction f_R with crystallinity, then the third term in the brackets is merely the fractional change in f_R with temperature. The data shown in *Figure 5* for the oriented sample yield 3.8×10^{-3} K^{-1} for this term, predicting a contribution to Υ of -133 μC m^{-2} K^{-1}. Clearly, as found previously for the homopolymer[1], this is much larger than the observed total response.

This is an overestimate for at least two reasons, however. In the first place, the measurement of crystallinity change is on a very slow timescale since the acquisition of n.m.r. data at one temperature typically takes 30 min or so but the pyroelectric coefficient was measured by oscillating the temperature of the sample with a period of 100 s. Clearly, a much smaller crystallinity change might be expected on this timescale. Also, we have assumed that when chains melt they completely lose their orientation and, conversely, when they crystallize they go from a random orientation to the average crystalline orientation. We might expect, however, that these changes occur near crystal surfaces where there is partial alignment of the non-crystalline phase and a smaller change in orientation is experienced on crystallization or melting.

Despite these problems, the magnitude of the observed crystallinity change is such that this must be considered a significant contribution to the observed pyroelectric coefficient.

CONCLUSIONS

A procedure has been devised for modelling the rigid lattice n.m.r. lineshape of the VDF/TrFE copolymer and used as the basis of decomposition of the composite n.m.r. signal into two components.

As with the homopolymer of PVDF[1], the rigid mass fraction f_R has been found to decrease reversibly with increasing temperature and calculations show that this could be a significant contribution to the pyroelectric coefficient.

In addition, an estimate of the increasing librational movement of the crystalline chains with increasing temperature has been obtained, and this also has been shown to make a significant contribution to the pyroelectric coefficient.

REFERENCES

1 Clements, J., Davies, G. R. and Ward, I. M. *Polymer* 1985, **26**, 208
2 Higashihata, Y., Sako, J. and Yagi, T. *Ferroelectrics* 1981, **32**, 85
3 Ohigashi, H. and Koga, K. *Japan. J. Appl. Phys.* 1982, **21**, L455
4 Yamada, T., Ueda, T. and Kitayama, T. *J. Appl. Phys.* 1981, **52**, 948
5 Nakagawa, K. and Ishida, Y. *J. Polym. Sci., Polym. Phys. Edn.* 1973, **11**, 2153
6 Yagi, T. *Polym. J.* 1980, **12**, 9
7 Andrew, E. R. *Phys. Rev.* 1953, **91**, 425
8 Pranadi, H. and Manuel, A. J. *Polymer* 1980, **21**, 303
9 Bevington, P. R. 'Data Reduction and Error Analysis for the Physical Sciences', McGraw-Hill, New York, 1969
10 Van Vleck, J. H. *Phys. Rev.* 1948, **74**, 1168
11 McBrierty, V. J. and Ward, I. M. *J. Phys. (D) Appl. Phys.* 1968, **1**, 1529
12 Hasegawa, R., Takahashi, Y., Chatani, Y. and Tadokoro, H. *Polym. J.* 1972, **3**, 5, 660
13 Tashiro, K., Takano, K., Kobayashi, M., Chatani, Y. and Tadokoro, H. *Polym. Prep. Japan* 1982, **31**, 2887
14 Folkes, M. J. and Ward, I. M. *J. Mater. Sci.* 1971, **6**, 582
15 Andrew, E. R. *J. Chem. Phys.* 1950, **18**, 607
16 Tashiro, K., Takano, K., Kobayashi, M., Chatani, Y. and Tadokoro, H. *Polymer* 1984, **25**, 195
17 Day, J. A. Ph.D. Thesis, Leeds University, 1990